第30卷第5期
2011年10月

红外与毫米波学报
J. Infrared Millim. Waves

Vol. 30, No. 5
October, 2011

文章编号:1001 - 9014(2011)05 - 0390 - 06

# Novel design of compact microstrip diplexer based on fractal-shaped composite right/left handed transmission line

XU He-Xiu, WANG Guang-Ming, ZHANG Chen-Xin, LIANG Jian-Gang
(Applied Microwave Laboratory, Missile Institute of Air Force Engineering University, Xi'an 713800, China)

**Abstract**: A new type of miniaturized microstrip diplexer is initially proposed based on the combined technology of fractal geometry and composite right/left handed transmission line (CRLH TL). The diplexer which is synthesized by combining two 3-port networks operating at a pair of different frequencies consists of lumped elements for the left handed (LH) part and Sierpinski-shaped microstrip lines (MLs) for the right handed (RH) part. Sierpinski curve allows miniaturized dimensions of the diplexer mainly attributing to its strong space-filling capability. CRLH TL enables dual-band design due to its unique hyperbolic-linear dispersion relation. For demonstration, three CRLH diplexers using Siepinski curves of different iteration orders are successfully designed. For verification, a CRLH diplexer sample by adopting a Sierpinski curve of second order was fabricated and measured. Consistent numerical and experimental results have confirmed the design. The fabricated diplexer operating at 0.9 and 1.8 GHz, respectively achieves good in-band performances and a maximal 76.3% size reduction compared to the conventional CRLH diplexer without fractal geometry.

**Key words**: Fractal, Space-filling property, Composite right/left-handed transmission line, Diplexer, Dual-band, Hyperbolic-linear dispersion relation
**PACS**: 40.41.20.Jb, 40.41.20. - q

# 基于分形复合左右手传输线的小型化微带双工器设计

许河秀, 王光明, 张晨新, 梁建刚
(空军工程大学导弹学院微波应用实验室,陕西 西安 713800)

**摘要**:基于分形几何与复合左右手传输线的混合技术方法,提出了一种新型小型化微带双工器并对其进行了研究。该双工器将工作于一对不同频率的两个三端口网络进行合成,由构成其左手部分的集总元件和右手部分的Sierpinski分形微带线组成。双工器的小型化得益于Sierpinski分形曲线的空间填充特性。而双工器的双频特性是由于复合左右手传输线具有双曲色散关系。为验证所提方法的有效性,成功设计了基于不同Sierpinski迭代次数的双工器。为证实仿真结果,加工测试了基于Sierpinski二次迭代分形的复合左右手双工器。仿真结果与测试结构吻合的很好。与未采用分形结构的传统复合左右手双工器相比,所制作的双工器工作于GSM两个频段(0.9和1.8 GHz)并获得了良好的通带性能和小型化比例,最大小型化比例达76.3%。

**关 键 词**:分形;空间填充特性;复合左右手传输线;双工器;双频;双曲色散关系
**中图分类号**:TN817;TN62 **文献标识码**:A

## Introduction

Left-handed (LH) metamaterial (MTM) has not become a particular hot topic and aroused much interest until its first fabrication in 2000[1]. As to the bulk MTM, there was still a long way before its practical

**Received date**: 2010 - 04 - 20, **revised date**: 2010 - 12 - 05 **收稿日期**:2010 - 04 - 20, **修回日期**:2010 - 12 - 05
**Foundation item**: Supported by National Natural Science Foundation of China (NO. 60971118) and 973 Project of Science and Technology Ministry of China (NO. 2009CB613306)
**Biography**: XU He-Xiu, male, Xi'an, China, PhD. Research field is fractal-shaped CRLH TL metamaterials and its application in circuits and antennas design. E-mail: hxxu20008@yahoo.cn.

application in microwave engineering since it featured large dimensions, complex structure, narrow band and large transmission loss, etc. In view of them, Eleftheriades[2] and Caloz[3] almost simultaneously proposed another type of LH MTMs based on the composite right/left-handed transmission line (CRLH TL). As exposed to the fractal geometry, it combining with electromagnetic theory has led to a wide application in the design of microwave components and antennas and enabled the compact[4], multiband[5] or wideband[6] design attributing to two most important aspects, i. e., the space-filling property and the self-similarity property. Most recently, fractal geometry has been employed in the design of complementary split ring resonators (CSRRs)[7-8] to form electrically smaller resonate-type LH sub-wavelength particles.

Conventional diplexers which are mainly adopted to make the receiver and transmitter share a common antenna consist of band-pass and band-stop filters, and thus are typically characterized by large dimensions. Hybrid diplexer is one type of classical configurations, however, it suffers large insertion loss, deteriorative isolation and is even not compact enough for modern wireless communication. Although a diplexer concentrating on the compact issue has been reported based on the multilayered LH transmission line (TL)[9], the particular fabrication process has brought us other issues of high cost and design complexity which have extremely limited its popularization in microwave engineering. To our relief, planar microstrip diplexer employing CRLH TL has been proposed to ease the fabrication[10].

The goal of this paper is to exploit a novel technology (fractal geometry combined with CRLH TL) to develop a compact diplexer with comprehensive performance as well as easy realization. The paper is organized as follows. In section 1, novel fractal-shaped diplexers are proposed, and also the corresponding theory in conjunction with the design procedures are derived. In section 2, the performances of the designed diplexers are assessed through illustrative results of simulation and measurement. Finally, a major conclusion is highlighted in section 3.

## 1 Proposed diplexer

The proposed microstrip diplexer in this work is synthesized based on standard printed circuit board (PCB) fabrication process. It combines two conventional 3-port networks (denoted as network$_1$ and network$_2$, respectively) operating at a pair of arbitrary frequencies. Although this concept was initially proposed in Ref. [10], the design procedure was not clear and the absence of implementation of the third TL section had reduced its technical merits. In this regard, the paper can be considered as a complete extension of [10] in theory and design. In this article, two target bands are specified as 0.9 GHz (with angular frequency denoted as $\omega_L$) and 1.8 GHz (with angular frequency denoted as $\omega_H$), respectively for practical application.

### 1.1 Major principle

A lossless reciprocal 3-port network has two most important characteristics. First, three ports are impossible to be matched simultaneously at any given band. Second, any two ports can be matched and let the residual one mismatched completely. In other words, there should be only one port through while the residual port is isolated when port 1 is excited. For analysis convenience, TL section between port 1 and port 2 is denoted as section I, whereas TL section between port 1 and port 3 is section II and the residual section between port 2 and port 3 section III. The novel designed 3-port network which is a combination of network$_1$ and network$_2$ should exhibit performances corresponding to those of the networks operating at $\omega_L$ and $\omega_H$, respectively. At $\omega_L$, port 1 and port 2 of the designed network are through while port 3 is isolated, which corresponds to the performance of network$_1$. Consequently the following expressions should be compulsorily satisfied.

$$\varphi_{x1} + \varphi_{x2} + \varphi_{x3} = 360n_1 \quad , \tag{1a}$$

$$\varphi_{x1} + \varphi_{x2} - \varphi_{x3} = 180 \times (2n_2 + 1) \quad . \tag{1b}$$

Note that $\varphi_{x1}$, $\varphi_{x2}$ and $\varphi_{x3}$ are electrical lengths of section Ⅰ, Ⅱ, Ⅲ at $\omega_L$, respectively. At $\omega_H$, port 1 and port 3 are through while port 2 is isolated, which relates to the performance of network$_2$. Equations similar to Eq. (1) are formulated as

$$\varphi_{y1} + \varphi_{y2} + \varphi_{y3} = 360n_3 \quad , \tag{2a}$$

$$\varphi_{y1} + \varphi_{y3} - \varphi_{y2} = 180 \times (2n_4 + 1) \quad . \tag{2b}$$

$\varphi_{y1}$, $\varphi_{y2}$ and $\varphi_{y3}$ are electrical lengths of section Ⅰ, Ⅱ, Ⅲ at $\omega_H$, respectively. Note that $n_1$, $n_2$, $n_3$ and $n_4$ are uncertain variables and can be selected as identical values.

Referring to above equations, there are ten unknowns while only four equations. Consequently, the solving process is impossible to be performed and in turn allows us several degrees of freedom which may be exploited to meet miniaturization and other technological requirements. To ease the design and fabrication, it is no need to implement the section Ⅲ by loading lumped-element CRLH TL. By contrast, a pure right-handed (RH) TL (microstrip line, ML) is enough. To this end, length and width of section Ⅲ are given in advance. Although the physical parameters of the section Ⅲ can be arbitrary in theory, the improper choice may lead to a large dimension of the final diplexer and even result in no solution to Eqs. (1) and (2).

In this paper, the length of section Ⅲ is carefully chosen as 51mm. With the fixed physical length, $\varphi_{x3}$ and $\varphi_{y3}$ can be calculated through commercial circuit simulator Ansoft Senerade according to the required characteristic impedance, the dielectric constant and height of applied microstrip substrate. The selection of $n_1$, $n_2$, $n_3$ and $n_4$ are cautiously performed by taking miniaturization into consideration. With the decided $\varphi_{x3}$, $\varphi_{y3}$, $n_1$, $n_2$, $n_3$ and $n_4$, values of $\varphi_{x1}$, $\varphi_{y1}$, $\varphi_{x2}$ and $\varphi_{y2}$ are immediately obtained according to Eqs. (1) and (2). It is worth to mention that $\varphi_{x1}$, $\varphi_{y1}$, $\varphi_{x2}$ and $\varphi_{y2}$ also can be determined by a separate optimization of network$_1$ and network$_2$ in Ansoft Serenade to make them exhibit specified electrical performances at $\omega_L$ and $\omega_H$, respectively. Because of the hyperbolic-linear dispersion relation of CRLH TL, section I and section Ⅱ with fixed phase responses can be synthesized by two different CRLH TLs, respectively. For simplicity, each of these two CRLH TLs is realized by only one CRLH cell. For good impedance match, the characteristic impedance $Z_c$ of these three TL sections should be twice the termination port impedance $Z_0$.

### 1.2 CRLH TL realization

In balanced condition, the CRLH cell, formed by a LH inductance $L_L$ in parallel with a parasitic RH capacitor $C_R$ in shunt branch and a LH capacitor $C_L$ in series with a RH inductor $L_R$ in series branch, can be decoupled into separate LH and RH subcircuits, which brings much convenience to the individual design of LH part and RH part. In current design, the LH part is engineered by artificially loading lumped elements based on surface mount technology (SMT) while the RH part is realized by MLs. The phase shift $\varphi^{CRLH}$ (electrical length) of a CRLH TL comprises a LH contribution $\varphi^{LH}$ and a RH contribution $\varphi^{RH}$.

$$\varphi^{CRLH} = \varphi^{LH} + \varphi^{RH} = \frac{N}{\omega\sqrt{L_L C_L}} - N\omega\sqrt{L_R C_R} \quad . \tag{3}$$

Where $N$ is the number of applied CRLH cells. For the sake of impedance match, the following expression is formulated

$$Z_c = \sqrt{\frac{L_R}{C_R}} = \sqrt{\frac{L_L}{C_L}} = 2Z_0 \quad . \tag{4}$$

The phase response and characteristic impedance of novel CRLH diplexers should be the same with those of conventional network$_1$ and network$_2$ operating at $\omega_L$ and $\omega_H$, respectively.

$$\varphi^{CRLH}(\omega = \omega_L) = \varphi_x \quad , \tag{5a}$$

$$\varphi^{CRLH}(\omega = \omega_H) = \varphi_y \quad . \tag{5b}$$

Insert Eq. (3) into Eq. (5), and then with the help of Eq. (4), values of the needed lumped elements are derived after some manipulations[3]

$$L_R = \frac{Z_c\left[\varphi_x\left(\frac{\omega_L}{\omega_H}\right) - \varphi_y\right]}{N\omega_H\left[1 - \left(\frac{\omega_L}{\omega_H}\right)^2\right]} \quad , \tag{6a}$$

$$C_R = \frac{\varphi_x\left(\frac{\omega_L}{\omega_H}\right) - \varphi_y}{N\omega_H Z_c\left[1 - \left(\frac{\omega_L}{\omega_H}\right)^2\right]} \quad , \tag{6b}$$

$$L_L = \frac{NZ_c\left[1 - \left(\frac{\omega_L}{\omega_H}\right)^2\right]}{\omega_L\left[\varphi_x - \varphi_y\left(\frac{\omega_L}{\omega_H}\right)\right]} \quad , \tag{6c}$$

$$C_L = \frac{N\left[1 - \left(\frac{\omega_L}{\omega_H}\right)^2\right]}{\omega_L Z_c\left[\varphi_x - \varphi_y\left(\frac{\omega_L}{\omega_H}\right)\right]} \quad . \tag{6d}$$

With values of $L_R$ and $C_R$, the necessary electrical length of RH ML is immediately calculated as

$$\varphi^{RH} = -N\omega_L\sqrt{L_R C_R} \quad , \tag{7}$$

To maintain $L_R$, $C_R$, $L_L$ and $C_L$ positive, $\varphi_x$ and $\varphi_y$ should satisfy the following two requirements, namely $\varphi_x\omega_L \geqslant \varphi_y\omega_H$, and $\varphi_x\omega_H \geqslant \varphi_y\omega_L$. Otherwise $\varphi_x$ should be added by $2\pi$ and then is repeatedly inserted into Eq. (6) to calculate values of lumped elements. Following above processes, values of the SMT elements constructing section I and section II are achieved. For symmetry and improved transmission performance, the T-type circuit as can be observed in the forthcoming Fig. 6 is terminated in two capacitors of $2C_L$ in each side. Table 1 summarizes the predicted and the used physical parameters of the designed CRLH diplexer. As is shown, there is an unavoidable discrepancy between them because the marketable SMT elements are available in discrete values. Since SMT chip components naturally own RH parasitic effect which in turn induces a small phase delay, a reduction of ML is required for calibration in practice. That is why the practically used MLs are a little shorter than the theoretically predicted ones.

**Table 1　Physical parameters of the proposed CRLH diplexer**

**表 1　所提出复合左右手传输线双工器的物理参数**

| | TL section | Inductor /nH | Capacitor ($2C_L$)/pF | RH TL length/mm |
|---|---|---|---|---|
| Theoretically predicted | Ⅰ | 57.5 | 11.5 | 128.4 |
| | Ⅱ | 94.5 | 18.9 | 61.4 |
| Practically used | Ⅰ | 56 | 12 | 127.5 |
| | Ⅱ | 100 | 18 | 60.5 |

### 1.3　Fractal implementation

The proposed CRLH diplexer is constructed as a Sierpinski curve of different iteration order (IO) from the point of view of miniaturization. Novel Sierpinski-shaped diplexers are fabricated on the Teflon substrate with a dielectric constant of $\varepsilon_r = 2.65$ and a thickness of $h = 1$ mm. Width of ML $W$ is set to be 0.75 mm corresponding to 100Ω. The Sierpinski curve is specified by its iteration factor (IF) and IO, whereas the IF represents the construction law or initiator of the fractal geometry and the IO indicates how many iteration processes have been carried out. In current design, Sierpinski curves of different IO are with identical initiator, namely the same IF. It has been well established that an incremental IO would result in smaller fractal segments and a smaller space between adjacent TLs. Consequently, there should be a tradeoff between the overall performance and the miniaturization of the diplexer as significant coupling between adjacent TLs in a finite space will deteriorate the performance. In this regard, the maximum IO is confined to the second.

Since many segments are introduced in the fractal implementation, right-angle or chamfered bends are commonly used to connect these fractal segments. Note that it is just these bends resulting in discontinuities of the surface current. The non-negligible discontinuity reactance which is associated with the phase-shifting property of fractals must be properly evaluated if one wants to exactly design fractal-shaped ML with a fixed phase. The reactance of each bend is modeled by a T-type circuit with an inductance $L_b$ in series branch and a capacitance $C_b$ in shunt branch. As to the right-angle bends used in the designed diplexers, the reactance of each one can be assessed by the following analytical close-form equations[11].

$$\frac{C_b}{W} = \frac{\left[\left(14\varepsilon_r + 12.5\right)\frac{W}{h} - \left(1.83\varepsilon_r - 2.25\right)\right]}{\sqrt{\frac{W}{h}}} + \frac{0.02h\varepsilon_r}{W} \quad , \tag{8a}$$

$$\frac{L_b}{h} = 50\left(4\sqrt{\frac{W}{h}} - 4.21\right) \quad . \tag{8b}$$

With computed $L_b$, $C_b$, the electrical length of the equivalent ML corresponding to the effect of discontinuities can be evaluated by Eq. (7) and the correlative physical length $L_f$ is finally synthesized in Ansoft Serenade. Note that $N$ in Eq. (7) for this purpose is the number of total fractal bends. To maintain the same electrical characteristics, the RH part of the designed CRLH TL should be shortened by $L_f$ for fractal implementation. Hence the overall circuit size is further reduced.

Fig. 1 shows the layout of the proposed fractal-shaped CRLH diplexers based on Sierpinski curves of zeroth, first and second IO, respectively. As can be observed, novel diplexers are more compact in size as IO increases. Compared to zeroth-order diplexer whose effective occupied area is $\pi \times 38.9 \times 38.9$ mm$^2$, the area of the first-order diplexer ($59.7 \times 59.7$ mm$^2$) is reduced by

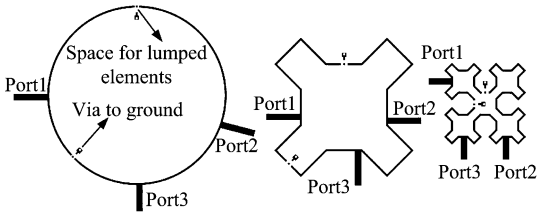


Fig. 1 Layout of proposed CRLH diplexer based on Sierpinski curves of (a) zeroth (conventional circular configuration) (b) first and (c) second iteration order, respectively
图1 所提出的基于不同迭代次数 Sierpinski 分形曲线复合左右手双工器的布局图 (a) 零次迭代(传统圆形布局) (b)一次迭代 (c)二次迭代

25.1%, whereas the miniaturization scale is 76.3% for the second-order diplexer ($33.6 \times 33.6$ mm$^2$).

## 2 Illustrative results

### 2.1 Numerical results

To validate the effectiveness of the combined technology, novel designed diplexers are analyzed by circuit simulation in Ansoft Serenade and by dynamic links and solver of planar EM and circuit co-simulation in commercial MOM (moment method)-based simulator Ansoft Designer. In co-simulation, the top-level circuit composed of SMT elements receives solution data from full-wave EM simulation of the subcircuit formed by MLs. Fig. 2 depicts the S-parameters of designed CRLH diplexer from circuit simulation, Fig. 3, Fig. 4 and Fig. 5 plots the full-wave S-parameters of the fractal-shaped CRLH diplexers of zeroth, first, and second order, respectively from co-simulation. Two most important aspects should be highlighted. Firstly, very obvious dual-band behavior around the GSM bands (centered at 0.9 and 1.8 GHz, respectively) can be observed. Consistent results obtained from Serenade and Designer have confirmed the design concept. Second, compared to the zeroth-order diplexer, the reflection and isolation performances of first- and second-order diplexers become a little worse attributing to discontinuity effect of the resultant much fractal bends. It seems that this effect enhances as IO increases and plays a more important role in affecting the upper band performances. Nevertheless, thanks to the correct design and exact evolution of the phase shifting of these bends, the two operating bands are almost without a frequency shift in all cases.

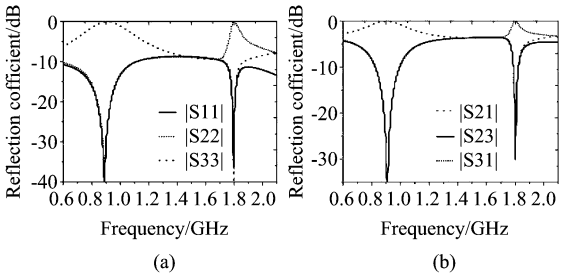


Fig. 2 S-parameters of designed CRLH diplexer from circuit simulation (a) reflection coefficient (b) transmission and isolation coefficient
图2 所设计复合左右手双工器的电路仿真S参数 (a)反射系数 (b)传输和隔离系数

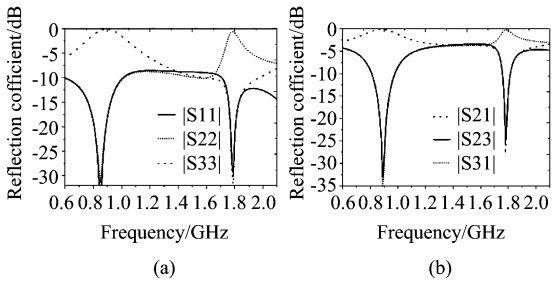


Fig. 3 S-parameters of the zeroth-order Sierpinski-shaped CRLH diplexer from EM and circuit co-simulation (a) reflection coefficient (b) transmission and isolation coefficient
图3 基于零次迭代 Sierpinski 复合左右手双工器的电磁和电路联合仿真S参数 (a)反射系数 (b)传输和隔离系数

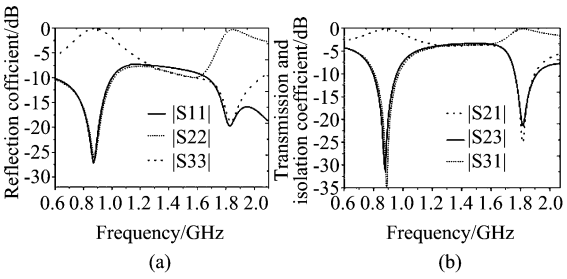


Fig. 4 S-parameters of the first-order Sierpinski-shaped CRLH diplexer from EM and circuit co-simulation (a) reflection coefficient (b) transmission and isolation coefficient
图4 基于一次迭代 Sierpinski 复合左右手双工器的电磁和电路联合仿真S参数 (a)反射系数 (b)传输和隔离系数

### 2.2 Experimental results

For verification, the second-order fractal-shaped CRLH diplexer has been fabricated and measured through Anritsu ME7808A vector network analyzer. Fig. 6 depicts the fabricated prototype of the diplexer. T-networks with chip capacitors and inductors of 0805 packages are adopted in the fabricated prototype. Fig. 7 displays the measured S-parameters of the second-

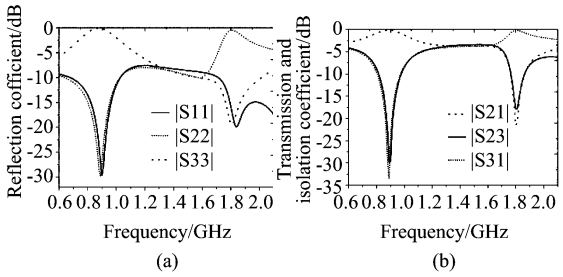


Fig. 5　S-parameters of the second-order Sierpinski-shaped CRLH diplexer from EM and circuit co-simulation (a) reflection coefficient (b) transmission and isolation coefficient
图5　基于二次迭代 Sierpinski 复合左右手双工器的电磁和电路联合仿真 S 参数 (a)反射系数 (b)传输和隔离系数

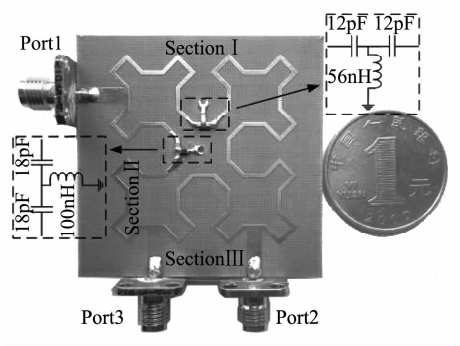


Fig. 6　Fabricated prototype of the designed second-order Sierpinski-shaped CRLH diplexer
图6　所设计的基于二次迭代 Sierpinski 复合左右手双工器的加工实物图

order fractal-shaped diplexer. Reasonable agreement between simulation (Fig. 5) and measurement (Fig. 7) can be observed in the whole frequency band of interest. Numerical and experimental results also reveal that port 2 is through at 0.9 GHz while port 3 is through at 1.8 GHz.

Referring to Fig. 7 (a), a slight frequency shift occurs in the fundamental lower band and can be observed from the measured reflection coefficient of port 1 and port 2. This discrepancy is mainly due to the applied none-ideal SMT components with value variation of ±10% in the fabricated prototype and partially attributable to the inherent tolerance in the fabrication process. From Fig. 7(b), it is obvious that the operating band characterized by isolation and insertion loss is with a slight frequency shift in the upper band, which can be successfully interpreted through the enhanced RH parasitical effect and the self resonance effect of SMT chip components in higher band. Nevertheless,

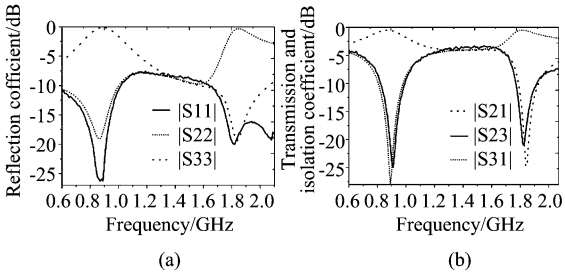


Fig. 7　Measured S-parameters of the second-order Sierpinski-shaped diplexer (a) reflection coefficient (b) transmission and isolation coefficient
图7　基于二次迭代 Sierpinski 复合左右手双工器的测试 S 参数 (a)反射系数 (b)传输和隔离系数

the measured frequency shift is within the scope of normal level.

In summary, measurement results indicate that: at 0.9 GHz, port 2 is through, $|S21| = -0.56$ dB, while port 3 is isolated, $|S31| = -25.5$ dB; at 1.8 GHz, port 3 is through, $|S31| = -0.53$ dB, while port 2 is isolated, $|S21| = -14$ dB. Moreover, the isolation coefficients $|S23|$ are $-23.99$ dB and $-15.9$ dB at 0.9 GHz and 1.8 GHz, respectively while the return loss $|S11|$ is better than 15 dB. In a word, it is obvious that the diplexer owns good performances, compact size and can successfully separate two different frequencies.

## 3　Conclusion

This paper exploits numerically and experimentally the concept of fractal-shaped CRLH TL in the synthesis of a set of novel compact diplexers. It has been demonstrated that fractal perturbation in CRLH TL does not result in any virulent deteriorative performance of the diplexers but leads to a significant size reduction. To the authors' s best knowledge, this is one of the simplest approaches among available data to design miniaturized diplexers by combining the techniques of fractal geometry and CRLH TL. It is thought that this concept shows potential application in modern miniaturized device and antenna design.

## REFERENCES

[1] Smith D R, Kroll N. Negative refractive index in left-handed materials[J]. *Phys. Rev. Lett.*, 2000, **85**: 2933 - 2936.

(下转 457 页)

(3) 棉花病害 SL 与 TM 影像光谱指数 B1,B3 和 RI 均呈极显著正相关,与 B4,OSAVI,MSAVI,TSAVI,SVNSWI,SNSWIa,SNSWIb,SVNI,DNSIa,DNSIb,NDSWIa,NDSWIb,RNSWIa,RNSWIb,DVNI,EVI,TVI,NDGI,SAVI,DVI,NDVI,RVI 和 PVI 均呈极显著负相关,与 SATVI 呈显著负相关,与 B2,B5 和 B7 均未达到极显著相关水平.

(4) 影像光谱指数 DVI 和 DNSIb 为变量的线性估测模型简单、实用、稳定性好,可作为 TM 卫星监测棉花黄萎病 SL 的最佳估测模型.

## REFERENCES


[1] LIU Zhan-Yu, Wang Da-Cheng, Li Bo, *et al*. Discrimination of lodged rice based on visible/near infrared spectroscopy[J]. *J. Infrared Millim. Waves*(刘占宇,王大成,李波,等. 基于可见光/近红外光谱技术的倒伏水稻识别研究. **红外与毫米波学报**),2009,**28**(5):342 - 345.

[2] BAI Jun-Hua, LI Shao-Kun, LI Jing , *et al*. Diagnosing cotton field quality with multi-temporal remote sensing data of cotton growth[J]. *Agricultural Sciences in china*(柏军华,李少昆,李静,等. 基于多时相棉花长势遥感的棉田质量诊断. **中国农业科学**),2008,**41**(4):1003 - 1011.

[3] Tilling A K, O'Leary G J, Ferwerda J G, *et al*. Remote sensing of nitrogen and water stress in wheat[J]. *Field Crops Research*2007,**104**(1):77 - 85.

[4] Huang W J, Lamb D W, Niu Z, *et al*. Identification of *yellow rust* in wheat using in-situ spectral reflectance measurements and airborne hyperspectral imaging[J]. *Precision Agriculture*2007,**8**(5):187 - 197.

[5] Johnson D A, Richard A J, Hamm P B, *et al*. Aerial photography used for spatial pattern analysis of *late blight* infection in irrigated potato circles[J]. *Phytopatholog*2003,**93**(7):805 - 812.

[6] Everitt J H, Escobar D E, Appel D N, *et al*. Using airborne digital imagery for detecting oak wilt disease[J]. *Plant disease*1999,**83**(6):502 - 505.

[7] Adams M L, Philpot W D, Norvell W A. Yellowness index: an application of spectral second derivatives to estimate *chlorosis* of leaves in stressed vegetation[J]. *International Journal of Remote Sensing*1999, **20** (18): 3663 - 3675.

[8] Hamid Muhammed H. Hyperspectral crop reflectance data for characterizing and estimating *fungal* disease severity in wheat[J]. *Bios stems Engineering*2005;**91**(1):9 - 20.

[9] Chen B, LI S K, Wang K R, *et al*. Spectrum characteristic of cotton canopy infected with Verticillium wilt and applications[J]. *Agricultural Sciences in china*2008,**7**(5):561 - 569.

[10] Apan A, Held A, Phinn S, *et al*. Detecting sugarcane '*orange rust*' disease using EO-1 Hyperion hyperspectral imagery[J]. *International Journal of Remote Sensing*, 2004,25(2):489 - 498.

[11] Jonas F, Gunter M. Multi-temporal wheat disease detection by multi-spectral remote sensing[J]. *Precision Agriculture*2007,**8**(3):161 - 172.

[12] Ma C. *Studying on Verticillium wilt and Fusarium wilt of cotton*[M]. Beijing: Chinese Agricultural Press(马存. **棉花枯萎病和黄萎病的研究**. 北京:中国农业出版社), 2007:158 - 161.


(上接 395 页)


[2] Grbic A, Eleftheriades G V. A backward-wave antenna based on negative refractive index L-C networks[C]. in Proc. IEEE-AP-S USNC/URSI National Radio Science Meeting, San Antonio,TX,2002:340 - 343.

[3] Caloz C, Itoh T. *Electromagnetic metamaterials: transmission line theory and microwave applications: the engineering approach*[M]. Wiley-Interscience publication, New York, 2006:197 - 198.

[4] Mario Barra, Carlos Collado, Jordi Mateu, *et al*. Miniaturization of superconducting filters using Hilbert fractal curves [J]. *IEEE Transactions on Applied Superconductivity*,2005, **15**:3841 - 3846.

[5] Jaume Anguera, Enrique Mart nez-Ortigosa, Carles Puente, *et al*. Broadband triple-frequency microstrip patch radiator combining a dual-band modified Sierpinski fractal and a monoband antenna[J]. *IEEE Trans Antennas Propag.*, 2006,**54**(11):3367 - 3372.

[6] Wen-Ling Chen, Guang-Ming Wang, Chen-Xin Zhang. Bandwidth enhancement of a microstrip-line-fed printed wide-slot antenna with a fractal-shaped slot[J]. *IEEE Trans Antennas Propag.*,2009,**57**(7):2176 - 2179.

[7] Vesna Crnojevic-Bengin, Vasa Radonic, Branka Jokanovic. Fractal geometries of complementary split-ring resonators [J]. *IEEE Trans Microw.* Theory Tech.,2008,**56**(10): 2312 - 2321.

[8] XU He-xiu, WANG Guang-ming, ZHANG Chen-xin, *et al*. Microstrip approach benefits quad splitter [J]. *Microwaves&rf*,2010,**49**(6):92 - 96.

[9] Horii Y, Caloz C, Itoh T. Super-compact multilayered left-handed transmission line and diplexer application[J]. *IEEE Trans Microw. Theory Tech*, 2005, **53** (4): 1527 - 1534.

[10] AN Jian, WANG Guang-ming, ZHANG Chen-xin, *et al*. Diplexer using composite right/left-handed transmission line[J]. *Electron Lett*,2008,**44**(11):685-U38.

[11] WANG Wen-Xiang. *Microwave engineering*[M]. Beijing: China National Defense Industry Press(王文祥. **微波工程技术**. 北京:国防工业出版社),2009:130 - 131.